IEEE Access
Multidisciplinary ⋮ Rapid Review ⋮ Open Access Journal

Received 29 August 2022, accepted 24 October 2022, date of publication 7 November 2022, date of current version 17 November 2022.

Digital Object Identifier 10.1109/ACCESS.2022.3219870

RESEARCH ARTICLE

High Precision Estimation of Laser FM-Noise Using RF Quadrature Demodulation Techniques

SEAN P. O'DUILL AND LIAM P. BARRY, (Senior Member, IEEE)
Radio and Optics Communications Laboratory, School of Electronic Engineering, Glasnevin, Dublin 9, D09 Y074 Ireland

Corresponding author: Sean P. O'duill (sean.oduill@dcu.ie)

This work was supported in part by the Science Foundation Ireland (SFI) co-funded under the European Regional Development Fund under Grant 18/EPSRC/3591 and Grant 12/RC/2276_P2, and in part by the European Space Agency under Contract 400012492018/NL/GLC/fk.

ABSTRACT We report on a technique that uses RF quadrature demodulation to measure laser FM-noise based on a delayed self-heterodyne setup. The measurement is self-referencing and the FM-noise can be measured with high precision over a sufficiently long duration that allows us to explore the limits imposed by the delay line in the well-known self-heterodyne laser phase noise measurement setup. We perform this measurement for two external cavity lasers with linewidths of tens of kilohertz and a fiber laser with a linewidth of 20 Hz. The scheme is checked and verified by finding good agreement between the FM-noise measured from beating the two external cavity lasers and the sum of the individual FM-noise of each laser.

INDEX TERMS Phase noise, lasers, spectral analysis, noise.

I. INTRODUCTION

Laser phase noise is an important quantity to gauge for applications that depend on the laser phase coherence [1], [2], [3]. For example, optical communications systems operating using coherent detection require lasers to have sub 100 kHz linewidths [4] and coherent LIDAR [5] also requires low phase noise sources, to name just a few. The laser spectrum is ideally a Lorentzian-broadened spectrum [1] and this spectrum can be quantified by a single metric, the width of the spectrum at the full width at half-maximum (FWHM). Ideally a laser with Lorentzian line-broadening has a flat FM-noise spectral density (SD) profile with a value in units of Hz^2/Hz and equaling the Lorentzian spectral FWHM value multiplied by 2π [1], [3]. However, electrically driven semiconductor lasers are also affected by low-frequency fluctuations in the central wavelength and hence these lasers have line-broadening beyond the Lorentzian lineshape, and the FM-noise SD is no longer flat [2], [3]. FM-noise SD is a superior method to gauge the laser phase noise characteristics, because the FM-noise SD resolves the dynamics of the FM-noise fluctuations in addition to quantifying the strength of the phase-noise [6]. Traditionally, the Lorentzian laser line-broadening spectrum can be measured using the delayed self-heterodyne (DSH) technique. The DSH technique is outlined in **Fig. 1**(a); the technique involves splitting the laser light into two paths with the light in one arm undergoing sinusoidal modulation to create a frequency translated copy of the original laser light, and the laser light in other path is delayed in an optical fiber. The light from both paths are then recombined and mixed on a photodiode. The Lorentzian linewidth is extracted by analyzing the spectrum of the mixing product from the photodiode. In the recent decade, improvements in high-resolution digital sampling and phase diverse optical coherent receivers have enabled the direct measurement of FM-noise. We list the FM-noise measurement techniques here: (i) laser FM-noise can be measured by mixing the laser light with an optical local oscillator and phase diversity receiver [6], [7]; (ii) a DSH method using strong phase modulation combined with a single photodetector and a digital storage oscilloscope (DSO) [8], we term that method the DSH-DSO technique; and (iii) a delayed self-homodyne (DSHo) phase diversity coherent receiver [8] which we term DSHo-DSO. These techniques require sampling at rates of the order of gigahertz to recover the optical field and hence extract the FM-noise SD. Moreover, since the FM-noise is based on averaging many fast-Fourier transforms (FFT) to ensure good precision in the FM noise SD calculations [9], the

The associate editor coordinating the review of this manuscript and approving it for publication was Luca Barletta.

high sampling rates and limited finite number of obtainable sampling points, implies a low precision of the FM-noise measurement.

One well-known issue associated with measuring the laser lineshape using the DSH method is that the fiber delay line limits the minimum linewidth that can be extracted [2]; the minimum linewidth being $\Delta f_{min} = (2\pi\tau_d)^{-1}$, where τ_d is the fiber delay duration. A question may arise as to how does the fiber delay impact on the FM-noise SD measurement, and to date there has been no study as to how the fiber delay line impinges on the FM-noise measurement using any DSH technique.

In this paper, we demonstrate two additional methods to measure the FM-noise SD of laser sources that have the highest precision to date. One method uses the internal in-phase (I) and quadrature (Q) sampling functionality commonly appearing in modern ESAs [10] and this method which we term DSH-IQ only requires a sampling rate at least two orders of magnitude smaller than the DSH-DSO method which in turn allows us to achieve two orders of magnitude better accuracy for a given number of samples. The other method makes use of the internal frequency down-conversion stages in the ESA to spectrally down-convert a heterodyne laser beat signal to be centered at 2 GHz for sampling using a DSO with a medium sampling rate of 10 GSa/s, while also achieving reasonable FM-noise accuracy when taking four million samples, as we were limited to in our experiment. The DSH-IQ method allows for much smaller sampling rates, in our case 100 MSa/s was more than sufficient. The lower sampling rate allows for the FM-noise SD to be measured at lower Fourier frequencies (f_F) for a given number of total acquired samples and/or the precision of the measurement to be much improved because of increased spectral averaging by calculating the FM-noise from many more shorter subset waveforms from the entire sampled waveform.

Moreover, the DSH-IQ method allows us to understand the limit imposed by the fiber delay line when measuring FM-noise SD using a self-referenced technique. We find that the limitation is completely different than that for the traditional swept spectrum technique for which delays shorter than the laser coherence time will result in multiple peaks appearing in the spectrum [2]. We find that while there is no imposed linewidth limit using any DSH-based FM-noise measurement; there is however a limitation to ensure that the duration of the temporal subset waveforms, to calculate each FFT, is less than the fiber delay. We demonstrate this for a fiber laser with a linewidth of 20 Hz.

This paper is organized as follows: in Section II we present linewidth results taken from the DSH method for three different lasers, two tunable laser sources and a fiber laser with 20 Hz linewidth. In Section III we present the DSH-IQ technique and present results confirming the linewidth results in Section II. In Section IV, we use ESA down-conversion to the 2 GHz intermediate frequency (IF) to analyze the heterodyne beat of the two tunable laser sources..

II. DSH METHODS

All of the measurement techniques in this paper are presented in **Fig. 1**. The DSH technique is outlined in **Fig. 1**(a), where the laser light is split equally along two paths [2], [3]. One path contains the fiber delay line and the light that travels along the other path undergoes frequency translation via sinusoidal modulation at a defined frequency f_T. The light from both arms is then coupled and mixed on a high speed photodiode with sufficient bandwidth (30 GHz) to capture the beat tone generated at f_T. The detected photocurrent I_{pd} is given as follows:

$$I_{pd} = \eta_{pd} |E_L(t)| |E_L(t-\tau_d)| \cos[2\pi f_T t + \phi_L(t) - \phi_L(t-\tau_d)] \quad (1)$$

where η_{pd} is the efficiency of the photodetector, E_L is the amplitude of the laser optical field of the laser, τ_d is the time delay of the fiber delay line. Since $|E_L(t)| \approx |E_L(t-\tau_d)|$, the main term of interest in (1) is the phase noise $\phi(t) - \phi(t-\tau_d)$, this is the term we wish to extract from I_{pd}. The photo- detected signal is then amplified by 20 dB using an RF amplifier before the ESA captures the beat signal using two possible methods. The traditional swept spectrum analysis method resolves the lineshape spectrum, by centering the ESA about f_T and measuring the power spectrum about a span wide enough to resolve the lineshape (ESA functionality for the swept spectrum technique is outlined in **Fig. 1**(c) (i)). Sufficient averaging is needed to remove random fluctuations about the beat spectrum, leaving a curve that can be fitted to a scaled Lorentzian lineshape function [1], [2], [3].

$$L_{DSH}(f) \propto \left[1 + \left(\frac{f - f_T}{\Delta f_L}\right)^2\right]^{-1} \quad (2)$$

For the case of the DSH method, the laser linewidth is $\Delta f_L/2$ because mixing the laser with a delayed copy of itself doubles the linewidth measured in the DSH setup. We used three different lasers for our experiments: two tunable laser sources and a fiber laser. TLS1 is an Emcore tunable laser of the type found in modern day coherent communication systems [4]. The second laser, termed TLS2 is a Photonetics tunable laser which is also an external cavity laser source. The fiber laser source (FLS) is a fiber laser from NKT photonics. The fiber delay line is 4.8 km length of dispersion shifted fiber which gives an approximate time delay of 24 μs. For the regular DSH method we take 100 spectral averages and fit the lineshape to a Lorentzian as described in (2). The DSH spectra of the three lasers are shown in **Fig. 2**. Both TLS lasers have a Lorentzian-like DSH spectrum; for TLS1 we find a linewidth of 13 kHz, and for TLS2 we find a linewidth of 27 kHz. Clear Lorentzian spectra are detected because the laser coherence time $t_{coh} = (2\pi\Delta f_L)^{-1}$ (maximum 14 μs) is shorter than the fiber delay. Issues arise for the FLS because no clear Lorentzian lineshape is visible (Fig. 2(c)) for the fiber laser whose coherence time (~20 ms) is obviously less than the fiber delay, hence the multiple peaks in the spectrum making any meaningful extraction of a Lorentzian linewidth

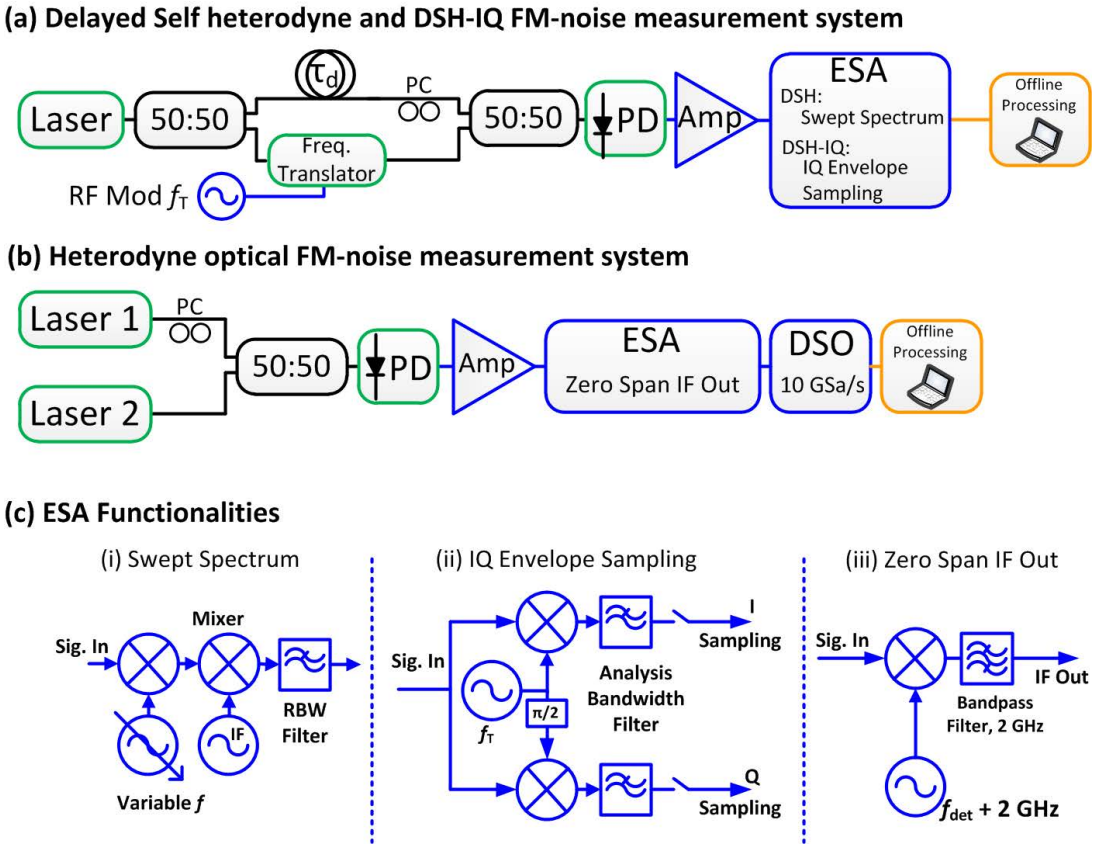

FIGURE 1. (a) Schematic of the DSH based linewidth and DSH-IQ FM-noise measurement systems. (b) Schematic of the heterodyne based FM-noise system. (c) Simplified ESA operation for: (i) swept spectrum, a tunable oscillator is tuned from f_T -Span/2 to f_T + span/2 and the power within the resolution bandwidth (RBW) is measured; (ii) fixed frequency with I-Q envelope sampling and (iii) zero-span intermediate frequency out (IF Out).

impossible, and none was attempted. Even though the swept spectrum approach failed for the FLS, we can still extract meaningful phase-noise metrics by analyzing the temporal waveform of $I_{pd}(t)$ using RF demodulation techniques from the ESA as outlined below.

III. THE DSH-IQ FM-NOISE MEASUREMENT TECHNIQUE

The DSH-IQ method is described as follows and the ESA functionality for this technique is outlined in **Fig. 1**(c) (ii). Instead of using the ESA to measure the spectrum by sweeping across a sufficiently wide frequency span to capture the spectrum, the ESA is operating as a quadrature demodulator of the envelope about the beat tone centered at f_T. The ESA is tuned to a fixed frequency f_T and then the ESA separates the envelope out into in-phase (I) and quadrature (Q) components, and both I and Q parts of the envelope are sampled simultaneously. The bandwidth of the IQ capture is limited to what is termed the analysis bandwidth, this is essentially the bandwidth of the resolution bandwidth filter (RBWF) within the ESA, because the ESA samples the signal at this point within the ESA detection process. Mathematically, the I and Q voltages detected by the ESA are:

$$\begin{aligned} V_I &\propto \left[I_{pd}(t) \times \cos(2\pi f_T t)\right] \otimes F_{AB}(t) \\ V_Q &\propto \left[I_{pd}(t) \times \sin(2\pi f_T t)\right] \otimes F_{AB}(t) \end{aligned} \tag{3}$$

these equations describes the entire process outlined in Fig. 1(c) (ii). $F_{AB}(t)$ is the impulse response of the analysis bandwidth filter, which is a sharp cut-off low pass filter. The operations in (3) move I_{pd} to baseband, and then the analysis bandwidth filters impose a strict bandwidth limit on the detection signal before sampling. Both V_I and V_Q are then sampled at sampling periods $t_S = R_S^{-1}$ with R_S being the sampling rate. The sampling process yields two sampled waveforms $V_{I,k}$ and $V_{Q,k}$ denoting the value of $V_{I,k}$ being the value of $V_I(kt_S)$(and similarly for $V_{Q,k}$). The phase information $\phi_L(t) - \phi_L(t - \tau_d)$ is now contained within the sampled envelope waveforms $V_{I,q}$ and $V_{Q,k}$.

Letting $\theta(k) = \phi_L(k) - \phi_L\left(k - \frac{\tau_d}{t_S}\right)$ be the phase at the k^{th} sample point, the instantaneous phase at each sample point is given by

$$\theta(k) = \text{detrend}\left(\text{unwrap}\left\{\tan^{-1}\left[V_{I,k}, V_{Q,k}\right]\right\}\right) \tag{4}$$

where the inverse tangent function is the two-argument inverse tangent function, the 'unwrap' operator removes phase discontinuities of 2π, and the 'detrend' operator removes the linear trend in the temporal phase which is equivalent to removing any remaining constant frequency offset. Once the phase has been extracted, the instantaneous

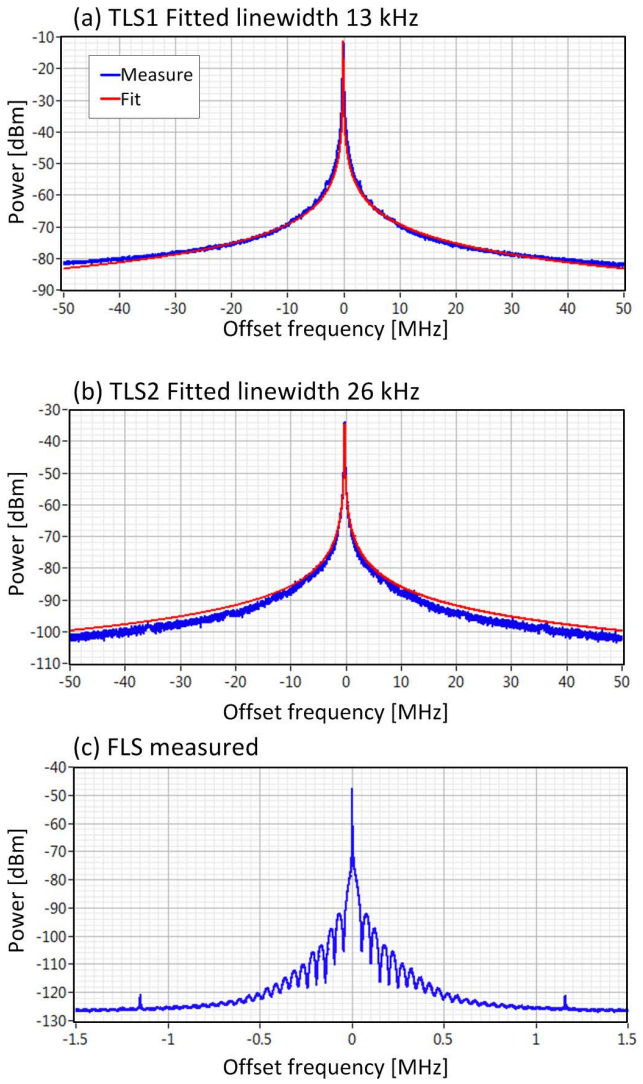

FIGURE 2. Measured and fitted Lorentzian lineshape function to (a) TLS1 laser. The fitted linewidth is 12.4 kHz. (b) TLS2 laser, the fitted lineshape is 27 kHz. (c) FLS, no attempt was made to fit this spectrum. In (b) The Lorentzian was fitted to the portion of the curve 30 dB down from the peak.

frequency at sample instance k is calculated by:

$$\Delta f\,(k) = \frac{R_S}{2\pi}\left[\theta\,(k+1) - \theta\,(k)\right] \tag{5}$$

The FM-noise of the laser is entirely encapsulated in the above equation. For an ideal laser, the laser would have a pure Lorentzian lineshape with spectral width at half maximum equal to Δf_L; correspondingly the FM-noise of an ideal laser would be flat with the value equal to $\Delta f_L / (2\pi)$. The spectral density estimate of the FM-noise can be done using Welch's method, where the averaged spectra of many shorter subsets of consecutive samples are taken from the entire sampled waveform

$$n_{FM}\,(m) = \eta_t \frac{2}{R_S N_{FFT}} \left\langle \left| \Delta\tilde{F}\,(m) \right|^2 \right\rangle \tag{6}$$

where $\Delta\tilde{F}\,[.]$ is the FFT operator, m is the FFT index, $\langle . \rangle$ denotes ensemble averaging of the number of FFTs calculated. The scaling within (6) converts the averaged FFT to the spectral density. Since the DSH-IQ method is self-referencing the measured FM-noise is double that of the laser, therefore $\eta_t = 0.5$ for the DSH-IQ method. For two laser heterodyning, the value of $\eta_t = 1$. The length of each waveform subset is given by N_{FFT} and the number of such waveform depends on the total number of samples taken, the number of samples taken within each FFT, N_{FFT}, and the percentage overlap between the subset waveforms. There is a tradeoff between the frequency granularity $\left(R_S / N_{FFT}\right)$ and the precision which is related to the number of averages in the ensemble averaging. For K averages of the FM-noise SD, the precision of the true FM-noise is contained within [9].

$$n_{FM}\,(k) = n_{FM,true}\,(k) \pm O\left[\sqrt{\frac{n_{FM}\,(k)}{K}}\right] \tag{7}$$

where $O\,(.)$ is 'order of' and is a shorthand for the uncertainty of the calculation of $n_{FM}\,(k)$, and as a rule of thumb the uncertainty reduces by the inverse square of the number of averages [8]. We obtain one million IQ samples of the DSH beat tone at a sample rate $R_S = 100$ MSa/s, using the ESA for the two tunable lasers (TLS1 and TLS2). The FM-noise is processed as per Eq. (4)-(6) and using N_{FFT} of 2,000 (20μs duration) with 75% overlap. For an immediate comparison with the fitted Lorentzian spectra and linewidth, we multiply all calculated FM-noise SD curves by 2π [6].

Before we present the FM-noise results, we demonstrate the importance of having an ideal optical frequency translation stage to make this scheme work. When modulating the laser light using sinusoidal modulation in **Fig. 1** (a), any remnant of the laser carrier or *both* first-order modulation sidebands (i.e. the sidebands for which the frequency difference between the sideband and the carrier equals the RF modulating frequency) causes the fundamental beat tone at f_T to comprise multiple beat products in the photo diode and destroys the ability to correctly extract the instantaneous phase. The DSH-DSO [8] method takes advantage of this because the envelope at f_T is multiplied by $\cos\left(\phi\,(t) - \phi\,(t-\tau_d)\right)$ and the first harmonic at $2\times f_T$ is multiplied by $\sin\left(\phi\,(t) - \phi\,(t-\tau_d)\right)$, that is why the DSH-DSO method needs to sample at multiples of $2\times f_T$. We found that an appropriately driven dual-drive MZM suppresses the carrier and one of the first-order sidebands and hence leaves the fundamental beat tone at f_T with constant amplitude; the schematic describing this frequency translator is given in Fig. 3(a). The spectrum confirming the absence of the carrier and sideband at $-f_T$ after the modulator is shown in Fig. 3(b). To present the modulator driving conditions we superimpose spectral results from a dual-drive MZM simulation where the output field from a dual-drive MZM is given by

$$E_o = E_i \frac{1}{2}\left(\exp\left[j\left(\frac{V_{RF_1}}{V_\pi}\cos\left(2\pi f_d t + \phi_{PS}\right) + \frac{V_{bias}}{V_\pi}\right)\right] + \exp\left[j\left(\frac{V_{RF_2}}{V_\pi}\cos\left(2\pi f_d t\right)\right)\right]\right) \tag{8}$$

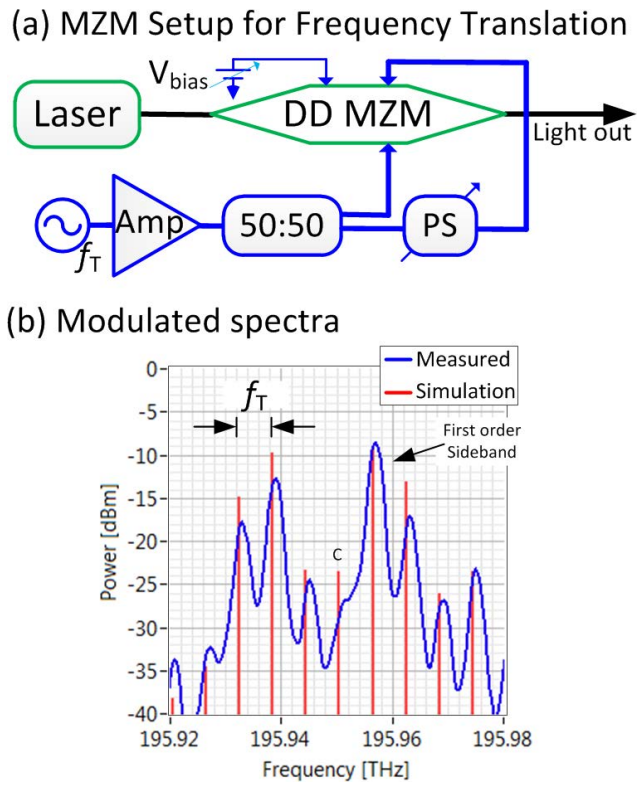

FIGURE 3. (a) Setup to frequency translate the laser field. A dual-drive Mach Zehnder (DD-MZM) is driven by two sinewaves, ideally one phase shifted by $\pi/2$. (b) The measured spectrum after the MZM. The carrier (C) and component at -6 GHz ($-f_T$) relative to the carrier are missing. PS denotes RF phase shifter. The simulation is used to extract approximate driving conditions.

where V_π is the voltage that induces a π phase shift in the travelling optical field. The RF source is sinusoidal with a frequency equal to the desired translation frequency f_T. Suppression of one of the first-order sidebands is achieved by inserting an RF phase shift of $\pi/2$ into one of the MZM arms; for low power modulation the carrier will not be suppressed though we find that increasing the RF power suppresses the carrier. The modulator driving conditions required are given in terms of V_π: $V_{RF_1} = 0.85V_\pi$, $V_{RF_2} = 0.7V_\pi$, $\phi_{PS} = 0.571\pi$ and $V_{bias} = 0.551V_\pi$.

The beat signal at the photodetector is generated by combining the light from the frequency translator stage with a delayed copy of the unmodulated carrier and mixing at the photodiode. The frequency translation stage ensures that there is only a single beat term that contributes to the beat signal at f_T. Even though there are multiple higher order modulation sidebands present arising from the modulation, the beat terms they generate with the delayed carrier are completely filtered out by the ESA analysis bandwidth filter and do not affect the FM-noise calculation. We show a 10,000-sample portion of the sampled waveforms and extracted instantaneous frequency in Fig. 4. The extracted instantaneous frequency results for the ideal frequency translation system are shown in Fig. 4(a)-(c); the results for the regular MZM modulation are shown in Fig. 4(d)-(f). With the ideal frequency translation system the I-Q vector in Fig.4 (a) traces out a circle with almost constant amplitude with the phase of each point being the phase noise from the laser, this is the exactly the photocurrent as described in (1). The instantaneous phase and frequency are then easily calculated. We note that the maximum frequency deviation in Fig. 4(c) is <1 MHz. However, the results change drastically for the case with regular MZM modulation when both first-order modulation sidebands are present, where the I-Q vector in Fig. 4(d) shows a random amplitude proportional to $\cos(\phi(t) - \phi(t - \tau_d))$ and phase with detrimental zero-crossings through the origin arising from the multiple contributions to the beat signal at f_T. The extracted phase in Fig. 4(e) shows discontinuities of almost 2π, and these discontinuities appear as sharp spikes (when differentiating the phase using (5)) in the instantaneous frequency plot in Fig. 4(f) and these large spikes can be upwards of 20 MHz in magnitude and corrupt the delicate FM-noise calculation.

The resulting FM-noise SD curves are shown in Fig. 5. To avoid confusion regarding definitions of frequency, we define the X-axis of FM-noise SD plots to be 'Fourier frequency'. Due to the limited ESA analysis bandwidth of 10 MHz, the FM-noise SD curves drop to zero for Fourier frequencies larger than 5 MHz. The FM-noise SD of TLS1 is found not to be constant and has a slight downward trend. The downward trend will be very useful when subsequently verifying this technique via the heterodyne method. The scaled FM-noise SD ranges from 40 kHz at a Fourier frequency of 50 kHz and decreases to below 10 kHz at a Fourier frequency of 5 MHz. For TLS1, we also plot the calculated FM-noise SD curve when regular MZM modulation is applied (i.e. both first-order modulation sidebands remain), this shows at least an order of magnitude error because of the extracted unphysical frequency spikes when estimating the instantaneous frequency. For TLS2 we find that for Fourier frequencies lower than 5 MHz the FM noise is flat with a scaled FM-noise SD equaling 28 kHz, which is very close to the value extracted from the Lorentzian fitting with the swept frequency scan in the previous subsection. The scaled FM-noise SD of the FLS presented in Fig. 5 reaches a minimum of 20 Hz and this is in line with FM-noise measurements taken using the DSH and strong PM scheme in [11] and <100 Hz as per the specifications from the manufacturer [12]. The apparent increase in FM-noise for the fiber laser measurement beyond Fourier frequencies of 1 MHz is due to the noise floor of the system caused by quantization noise in the ESA internal sampling and electrical noise in the amplifier and photodiode. We add a trend line proportional to f_F^2 to show that calculated FM-noise SD for the fiber laser reaches such a limit for Fourier frequencies >1 MHz. The fact that that portion of the FM-noise SD curve does not arise from laser phase fluctuations is confirmed in the next section when investigating the limits imposed by the fiber delay line on the FM-noise measurement.

We now explore the impact of increasing the number of N_{FFT} samples when calculating the FM-noise SD and increase the duration of each subset to be longer than the fiber

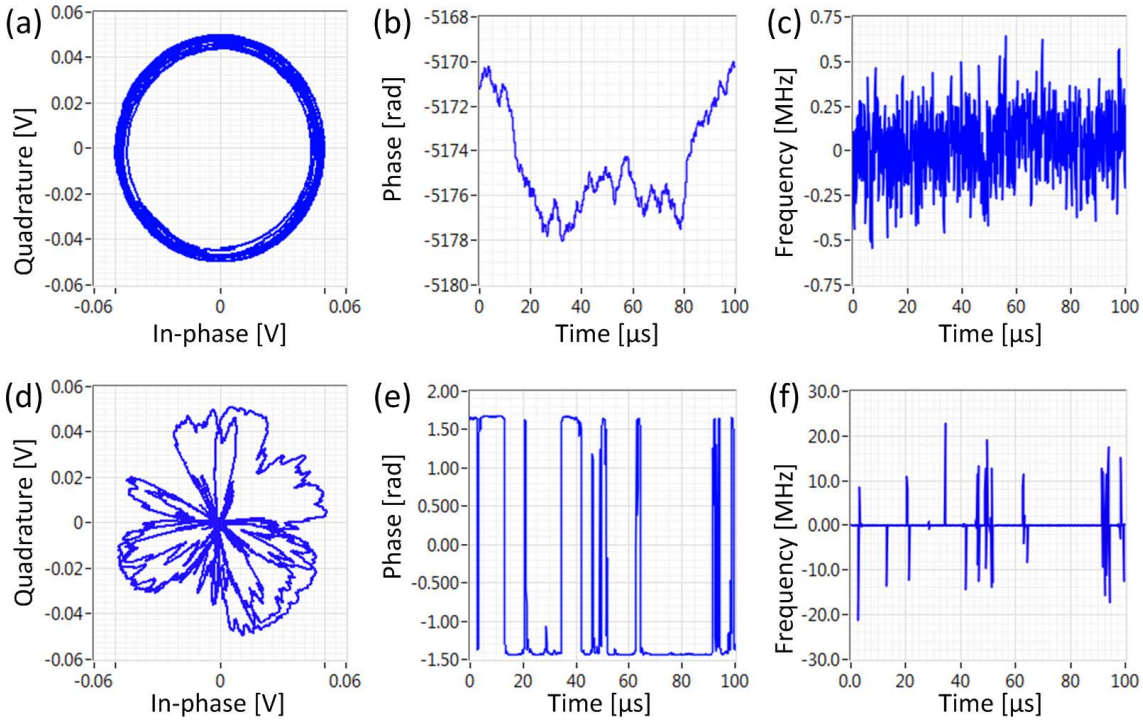

FIGURE 4. Plots of: the IQ-vector from quadrature demodulation (a) and (d); instantaneous phase (b) and (e), and instantaneous frequency in (c) and (f). Plots (a) –(c) are the plots for frequency translation, exact instantaneous frequency without spikes is obtained when the I-Q vector, plot (a), makes no transition through the origin. Plots (d)-(f) are for regular MZM modulation, multiple beat terms appear at the detector resulting in IQ transitions, plot (d), through the origin resulting in discontinuities of phase approaching 2π and hence sharp spikes in the instantaneous frequency giving incorrect values for the FM-noise SD.

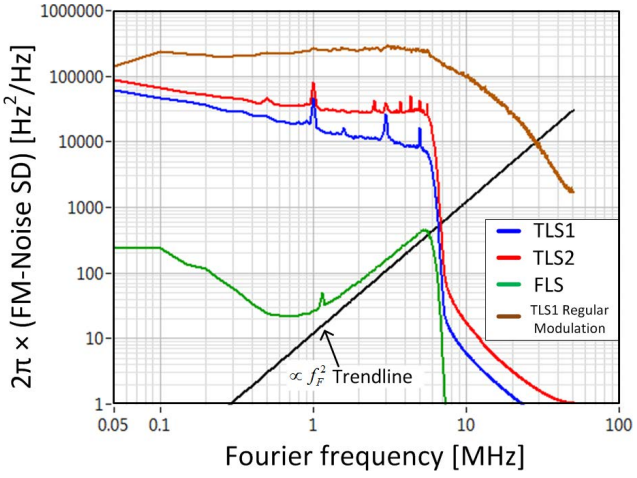

FIGURE 5. Measured FM-noise SD of the three lasers using the DSH-IQ method. The flatter portions of both agree with the respective Lorentzian linewidths 13 kHz and 27 kHz respectively. The onset of 1/f FM-noise is clearly visible. Also shown is the incorrect FM-noise SD measured when strict frequency translation is violated using regular MZM modulation. A trendline indicating a noise floor proportional to f_F^2 is included.

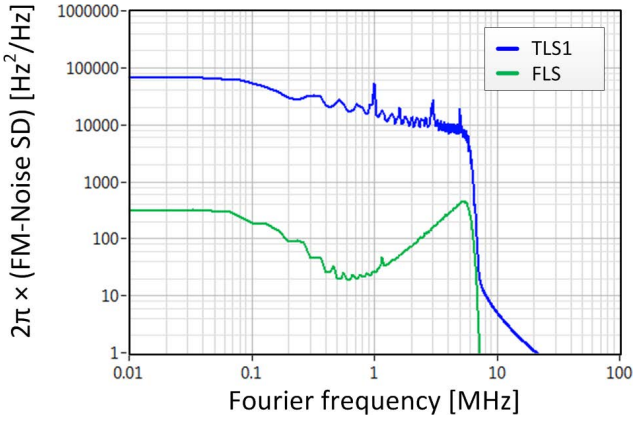

FIGURE 6. Measured FM-noise of TLS1 and FLS using subarrays whose duration exceeds the delay of the fiber delay line. Note the resulting comb-like ripple features in the spectra.

delay. This means that some of the phase samples re-appear at the end of the subset thus the phase waveform is no longer uncorrelated. For a 4.8km length of the fiber delay line the delay is ∼24 μs, therefore setting N_{FFT} to be 2,500, the duration of each sub waveform is now 25 μs (2,500/(100 × 10^6)s). Recalculating the FM-noise and displaying the results in Fig. 6, we find that increasing the effective duration of the subset arrays beyond the fiber delay results in comb-like ripples in the FM-Noise spectrum that vary about the actual FM-noise curve, increasing the effective duration of the array subsets only exacerbates the ripples and the presence of these ripples and can make an inference of FM-noise impractical. Therefore we have reached the restriction imposed by the fiber delay line. One point of interest is the FLS result; the increase in FM-noise SD beyond 1 MHz does not show any comb-like ripples therefore we can safely conclude that that portion of the curve arises from noise in the entire detection system and is unrelated to the phase noise

of the FLS. Note that with TLS1 for Fourier frequencies greater than 1 MHz, the FM-noise contains comb-like ripples, therefore we can conclude that there is minimal impact from the system noise in the FM-noise SD measurement of TLS1. We are able to reach the limit imposed by the fiber delay because we only need to sample the I-Q envelope of the beat tone at sub gigahertz sampling rates, and therefore we can detect waveforms of longer durations and average over many smaller subsets. It is important to note that the minimum measurable Fourier frequency equals the sampling rate divided by the number of elements in the FFT. So the choice of sampling rate and the maximum number of samples that the instrument can store over one sampling burst, will determine the minimum Fourier frequency. We recommend that the FM-noise curves should be averaged at least 10 times to lessen the uncertainty of the FM-noise measurement.

IV. FM-NOISE MEASUREMENT USING LASER HETERODYNING WITH ESA-ASSISTED DOWN-COWNVERSION AND DIGITIGAL SAMPLING

To verify the FM-noise results from the DSH-IQ method, we heterodyne TLS1 and TLS2 to see if the FM-noise of the heterodyne beat equals the sum of the individual FM-noise of the two lasers. The setup is shown in Fig. 1(b) where light from the two lasers is coupled together and the amplified beat tone is then detected using the ESA. The FM-noise of the heterodyne beat can be measured using quadrature I-Q demodulation as was done in [13]. The FM-noise can be measured in this way provided that the frequency drift of the lasers does not exceed the analysis bandwidth of the ESA. ESA's with analysis bandwidths exceeding 100 MHz are needed to capture the heterodyne beat without the slowly varying frequency drift from the laser technical noise moving the beat tone outside the analysis bandwidth. The maximum analysis bandwidth of our ESA was 10 MHz and this is much too low to capture the heterodyne beat tone. To overcome limitations imposed by the analysis bandwidth when using quadrature detection, we operate the ESA in zero span mode and process the signal at an intermediate frequency mixing stage within the ESA, where the beat tone has been mixed down and centered at 2 GHz with a total bandpass signal bandwidth of 2 GHz (i.e. the equivalent analysis bandwidth is 2 GHz in this case). The down converted 2 GHz signal is then sampled using a digital sampling oscilloscope (DSO) with no synchronization required between ESA and DSO. The voltage captured by the DSO is:

$$V_{DSO,k} = V_{DSO}(k\Delta t_S) \propto |E_{TLS1}(k\Delta t_S)|\,|E_{TLS2}(k\Delta t_S)| \times \cos\left[(2\pi)\left(2\times 10^9\right)k\Delta t_S + \phi_{TLS1}(k\Delta t_S) - \phi_{TLS2}(k\Delta t_S)\right] \quad (9)$$

For this scheme to work, the frequency difference between the lasers must be less than the PD bandwidth and the ESA must be able to tune to the beat frequency to down convert the signal to 2 GHz. Note, there may be a minimum frequency

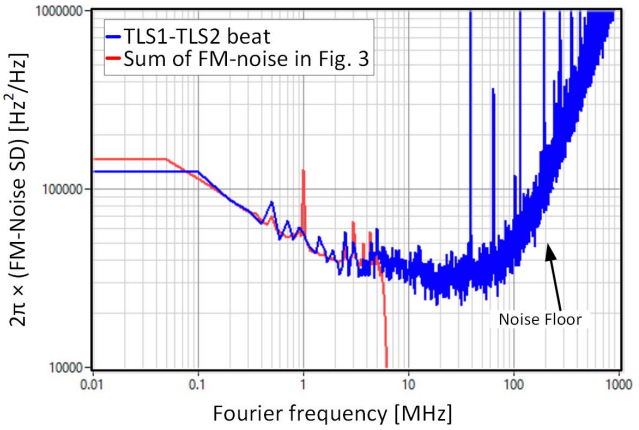

FIGURE 7. Measured FM-noise SD from the beat of TLS1 and TLS2. The measured curve coincides exactly with the summation of the individual FM noise SD curves of the two lasers.

that the ESA can down convert to 2 GHz, and for the ESA that we used the minimum down convertible frequency is 8 GHz. Resuming the analysis, we are interested in extracting the $\phi_{TLS1}(t) - \phi_{TLS2}(t)$ part of Eq. (9). This is done by converting the sampled signal to a complex-valued analytic signal. By setting $V_{I,k} = V_{DSO,k}$, the quadrature component is given by [14]

$$V_{Q,k} = H\left[V_{I,k}\right] \quad (10)$$

where $H[.]$ is the discrete Hilbert transform operator [15]. The phase and subsequently the FM-noise is then extracted using Eqs (4)-(6). The beat signal was sampled at 10 GSa/s using a Tektronix DSO with analogue bandwidth of 2.5 GHz. The FM-noise is then extracted from the samples and the FM-noise SD is calculated with a value of $N_{FFT} = 1 \times 10^5$. The FM noise of the beat signal between TLS1 and TLS2 is shown in Fig. 7. For the case of lasers with uncorrelated phase noise, the FM-noise of the beat equals the summation of the FM-noise of each individual laser. We also plot the summation of the FM-noise curves of each individual laser from Fig. 5, and the results over-lap excellently upto 5 MHz, which is the limit of the technique used to measure the FM noise using the DSH-IQ technique arising from the analysis bandwidth. The system noise creates a noise floor that appears at 100 MHz and then the FM-noise increases due to this system noise.

V. DISCUSSION AND CONCLUSION

We have presented with justifying results, methods to measure the FM-noise using RF quadrature demodulation techniques. The lower sampling rate of the DSH-IQ method presented allows us to calculate FM-noise with high precision and high accuracy down to Fourier frequencies imposed by the fiber delay line. The technique allows us to explore and understand the limitation imposed by the fiber delay line when calculating the FM-noise from DSH set-up, thus confirming the validity of measuring FM-noise of lasers with extremely low linewidth of tens of Hz using a DSH set-up,

even though prohibited by standard swept spectrum techniques. The value of the FM-noise SD calculated via the DSH-IQ method compares well with the traditional swept frequency spectrum and laser heterodyning methods. Although the analysis bandwidth of the ESA used in these measurements is 10 MHz, options are available to increase the analysis bandwidth to a few hundred megahertz and extend the FM-noise measurement to higher frequencies. In addition, other options for frequency translation are available instead of employing a dual-drive MZM, e.g. the method should work equally well if an acousto-optic modulator was used as the frequency translator instead, which may simplify the entire setup considerably. Since we have demonstrated a method that potentially can measure the FM-noise of lasers for Fourier frequencies below 1 kHz; improving the environmental isolation of the fiber reel when increasing the fiber length to measure the FM-noise SD at lower Fourier frequencies would be recommended [16], [17].

ACKNOWLEDGMENT

The authors are grateful to Dr. John Jost and Erwan Lucas of MicroR Systems for helpful discussions about quadrature demodulation and FM-noise analysis.

REFERENCES

[1] A. L. Schawlow and C. H. Townes, "Infrared and optical masers," *Phys. Rev.*, vol. 112, no. 6, p. 1940, 1958.
[2] H. Ludvigsen, M. Tossavainen, and M. Kaivola, "Laser linewidth measurements using self-homodyne detection with short delay," *Opt. Commun.*, vol. 155, pp. 180–186, Oct. 1998.
[3] G. Morthier and V. Vankwikelberge, *Handbook of Distributed Feedback Laser Diodes*, 2nd ed. Norwood, MA, USA: Artech House, 2013.
[4] A. Daiber, "Narrow-linewidth tunable external cavity laser for coherent communication," in *Proc. IEEE Photon. Conf.*, Dec. 2014, Paper WD3.1, doi: 10.1109/IPCON.2014.6995441.
[5] P. A. Morton, C. Xiang, J. B. Khurgin, C. D. Morton, M. Tran, J. Peters, J. Guo, M. J. Morton, and J. E. Bowers, "Integrated coherent tunable laser (ICTL) with ultra-wideband wavelength tuning and sub-100 Hz Lorentzian linewidth," *J. Lightw. Technol.*, vol. 40, no. 6, pp. 1802–1809, Mar. 15, 2022.
[6] K. Kikuchi, "Characterization of semiconductor-laser phase noise and estimation of bit-error rate performance with low-speed offline digital coherent receivers," *Opt. Exp.*, vol. 20, no. 5, pp. 5291–302, 2012.
[7] A. J. Walsh, J. A. O'Dowd, V. M. Bessler, K. Shi, F. Smyth, J. M. Dailey, B. Kelleher, L. P. Barry, and A. D. Ellis, "Characterization of time-resolved laser differential phase using 3D complementary cumulative distribution functions," *OSA Opt. Lett.*, vol. 37, no. 10, pp. 1769–1771, 2012.
[8] T. Huynh, L. Nyguyen, and L. P. Barry, "Delayed self-heterodyne phase noise measurements with coherent phase modulation detection," *IEEE Photon. Technol. Lett.*, vol. 24, no. 4, pp. 249–251, Oct. 31, 2012.
[9] P. D. Welch, "The use of fast Fourier transform for the estimation of power spectra: A method based on time averaging over short modified periodograms," *IEEE Trans. Audio Electroacoustics*, vol. AE-15, no. 2, pp. 70–73, Jun. 1967.
[10] P. Baudin, *Wireless Transceiver Architecture: Bridging RF and Digital Communications*. New Delhi, India: Wiley, 2014.
[11] T. Verolet, G. Aubin, Y. Lin, C. Browning, K. Merghem, F. Lelarge, C. Calo, A. Delmade, K. Mekhazni, E. Giacoumidis, A. Shen, L. Barry, and A. Ramdane, "Mode locked laser phase noise reduction under optical feedback for coherent DWDM communication," *IEEE J. Lightwav. Technol.*, vol. 38, no. 20, pp. 5708–5715, Oct. 15, 2020.
[12] *Koheras MIKRO—Single-Frequency OEM Lasers*. Accessed: Nov. 14, 2022. [Online]. Available: https://www.nktphotonics.com/products/single-frequency-lasers/koheras-mikro/
[13] N. G. Pavlov, J. He, R. N. Wang, J. Liu, A. S. Raja, G. Lihachev, R. Phelan, T. J. Kippenberg, and J. D. Jost, "Ultra-compact and ultra high–Q photonic chip based optical reference cavity at 1550 nm," in *Proc. OSA Laser Congr.*, Toronto, ON, Canadian, 2021, Art. no. JTu1A.51.
[14] G. Brajato, L. Lundberg, V. Torres-Company, M. Karlsson, and D. Zibar, "Bayesian filtering framework for noise characterization of frequency combs," *Opt. Exp.*, vol. 28, no. 9, p. 13949, 2020.
[15] R. N. Bracewell, *The Fourier Transform & Its Applications*. New York, NY, USA: McGraw-Hill, 1999.
[16] F. Kéfélian, H. Jiang, P. Lemonde, and G. Santarelli, "Ultralow-frequency-noise stabilization of a laser by locking to an optical fiber-delay line," *Optica Opt. Lett.*, vol. 34, no. 7, pp. 914–946, 2009.
[17] H. Tian, F. Meng, K. Wang, B. Lin, S. Cao, Z. Fang, Y. Song, and M. Hu, "Optical frequency comb stabilized to a fiber delay line," *Appl. Phys. Lett.*, vol. 119, no. 12, Sep. 2021, Art. no. 121106.

SEAN P. O'DUILL received the B.E. and Ph.D. degrees from University College Dublin, in 1999 and 2008, respectively. The work of the Ph.D. thesis concerned tunable laser characterization for dual-format signaling and for the impact of optical fiber nonlinearities on dual-format signals. From May 2008 to September 2011, he was a Postdoctoral Fellow at Technion working on slow light techniques for microwave signal processing and also for optical frequency comb generation. From October 2011 to October 2012, he was with the Karlsruhe Institute of Technology, developing theory and numerical simulation platforms of semiconductor optical amplifiers for use in passive optical networks and for all-optical signal processing. Since November 2012, he has been with the Radio and Optics Communications Laboratory, DCU, simulating performance capabilities of optical signal processing subsystems for use in future networks, and from August 2015 to December 2019, he received an SFI Industrial Fellowship to work part time designing lasers within a DCU spin-off company, Pilot Photonics Ltd.

LIAM P. BARRY (Senior Member, IEEE) received the B.E. degree in electronic engineering and the M.Eng.Sc. degree in optical communications from University College Dublin, in 1991 and 1993, respectively, and the Ph.D. degree from the University of Rennes, France. He was subsequently employed as a Research Engineer with the France Telecom's Research Laboratories (now known as Orange Laboratories), Optical Systems Department, and as a result of this work. In February 1996, he joined the Applied Optics Centre, Auckland University, New Zealand, as a Research Fellow and in March 1998, he took up a lecturing position with the School of Electronic Engineering, Dublin City University, and established the Radio and Optical Communications Laboratory. He is currently a Professor with the School of Electronic Engineering, a Principal Investigator at Science Foundation Ireland, a member of the Royal Irish Academy, a Board Member of the Irish Research Council, and the Director of the Radio and Optical Communications Laboratory. He has published over 500 articles in international peer-reviewed journals and conferences and holds ten patents in the area of optoelectronics. His research interests include all-optical signal processing and characterization, hybrid radio/fiber communication systems, wavelength tunable lasers for reconfigurable optical networks, and optical frequency combs for high capacity transmission systems. He was a TPC Member of the European Conference on Optical Communications (ECOC), from 2004 to 2018, and served as the ECOC Co-Chair for ECOC2019 in Dublin. He has also been a TPC Member of the Optical Fiber Communication Conference (OFC), from 2007 to 2010, serving as the Chair of the Optoelectronic Devices Sub-Committee for OFC 2010.